AJNR

Steady-state free precession imaging of the inner ear.

A E Stillman, K Remley, D J Loes, X Hu and R E Latchaw

AJNR Am J Neuroradiol 1994, 15 (2) 348-350
http://www.ajnr.org/content/15/2/348

Steady-State Free Precession Imaging of the Inner Ear

Arthur E. Stillman, Kent Remley, Dan J. Loes, Xiaoping Hu, and Richard E. Latchaw

Summary: The authors describe a steady-state free precession technique for imaging the inner ear. Although the signal-to-noise ratio is not as great as with other three-dimensional MR techniques, the inherent high contrast of inner ear structures makes this a valuable technique for patients with sensorineural hearing loss and for those who refuse paramagnetic contrast material.

Index terms: Magnetic resonance, technique; Magnetic resonance, 3-D; Ear, magnetic resonance

There has been recent interest in high-resolution imaging of the inner ear by three-dimensional magnetic resonance (MR) techniques (1, 2). These studies have demonstrated that such images improve visualization of inner ear anatomy compared with spin-echo MR and computed tomography of the temporal bone. Although these techniques have relatively good signal-to-noise ratios, the intrinsic contrast of the fluid-filled membranous labyrinth and neighboring neural tissues is low compared with T2-weighted spin-echo images. In this paper we propose steady-state free precession (3, 4) as an alternative means for imaging the inner ear. Although the signal-to-noise ratio is not as great as with the previous 3-D techniques, the inherent contrast of the inner ear structures is superior, permitting improved maximum-intensity projection reconstruction of the images similar to angiography. These projections may be viewed in any plane, to display the anatomy to greatest advantage. Moreover, multiplanar reformatting is possible.

Materials and Methods

All images were obtained on a 1.5-T imaging system (Magnetom SP; Siemens, Iselin, NJ) as part of our standard MR protocol for evaluation of the cerebellopontine angle and internal auditory canal. A standard circularly polarized quadrature head coil was used for most pulse sequences. Images were obtained in the coronal plane using the following parameters: 17/7/2 (repetition time/echo time/excitations), field of view of 200 mm, matrix of 256 × 256, flip angle of 90°, 32 partitions, and section thickness of 1.0 mm.

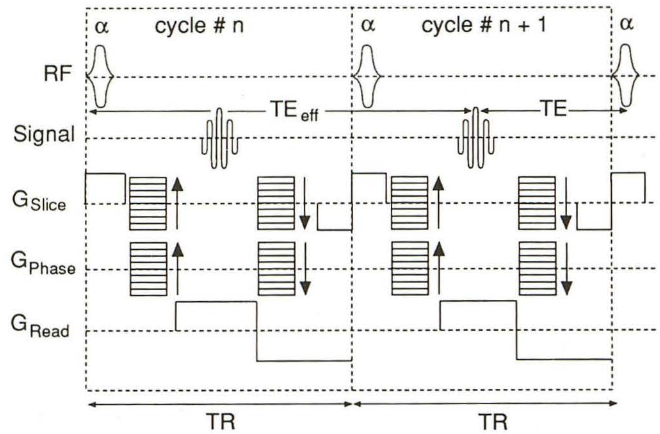

Fig. 1. Pulse sequence diagram for 3-D steady-state free precession. The effective echo time is given by $TE_{eff} = 2TR - TE$, giving rise to significant T2 weighting of the images.

More recently a modified pulse sequence was used to obtain greater spatial resolution with a 10-cm-diameter circular receive-only surface coil. Parameters used with this newer sequence were 19/8.3/4, field of view of 150 mm, matrix of 256 × 256 matrix, flip angle of 90°, 32 partitions, and section thickness of 0.9 mm. Both sequences used gradient-motion rephasing in the readout direction.

The steady-state free precession high-resolution sequences were performed after obtaining informed consent as part of a protocol approved by our institutional review board. More than 50 patients and 10 volunteers have been studied to date.

A schematic of the pulse sequence is shown in Fig 1. It is seen that the spins are refocused earlier by the gradients than the expected spin-echo by echo time. Thus the effective echo time is given by $TE_{eff} = 2TR - TE$. This leads to significant T2 weighting of the images. Cerebrospinal fluid and endolymph appear bright, whereas neural structures have low signal intensity.

Received July 14, 1992; accepted pending revision October 12; revision received December 29.

From the Department of Radiology, University of Minnesota, Minneapolis.

Address reprint requests to Arthur E. Stillman, MD, Department of Radiology, Box 292, University of Minnesota Hospital, 420 Delaware St SE, Minneapolis, MN 55455.

AJNR 15:348–350, Feb 1994 0195-6108/94/1502–0348

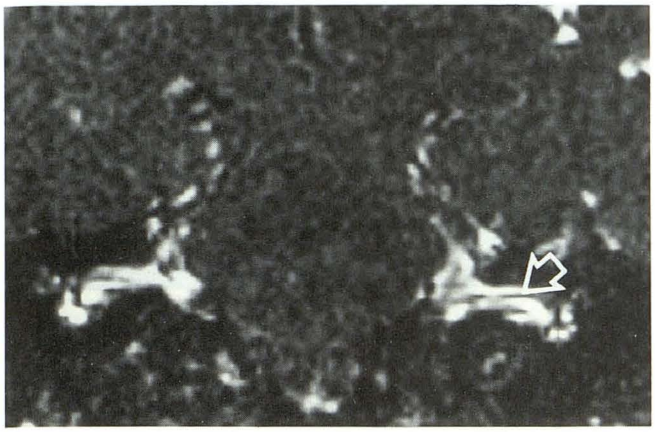

A

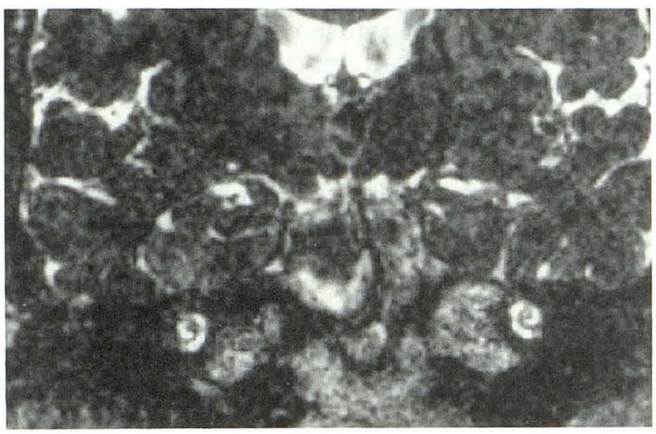

B

Fig. 2. Coronal steady-state free precession image of normal internal auditory canal (*A*) and cochlea (*B*). Cerebrospinal fluid and endolymph appear bright on these heavily T2-weighted images. The VII and VIII cranial nerve complex (*arrow*) is seen as a low-intensity structure within the internal auditory canal.

Fig. 3. Maximum-intensity projection reconstruction image of the internal auditory canal. These images provide a 3-D perspective of the membranous labyrinth when viewed by cine technique.

Results

Steady-state free precession is known to be motion sensitive. With the exception of several studies of very uncooperative patients, all images were judged to have adequate quality for evaluation.

Typical normal images are shown in Fig 2. Note that bright signal is present in the internal auditory canals, membranous labyrinth, cisterns, and brain sulci. The VII and VIII nerve complex consistently is observed as a low-intensity structure within the internal auditory canal. The cochlea, semicircular canals, and vestibule are likewise consistently visualized. These images lend themselves to maximum-intensity projection reconstructions similar to MR angiography; the structures of interest are bright, and there is good contrast with the surrounding tissue. A representative maximum-intensity projection reconstruction is shown in Fig 3. These images permit a 3-D of the membranous labyrinth, which is best appreciated when viewed with a cine technique. Using a surface coil, it is possible to obtain high-resolution images, and fine structures such as the cochlear aqueduct may be seen (Fig 4). Because the images are obtained in a 3-D data set, it is possible to reconstruct them in any plane using standard software. A sagittal reconstruction of a high-resolution surface-coil study of a healthy

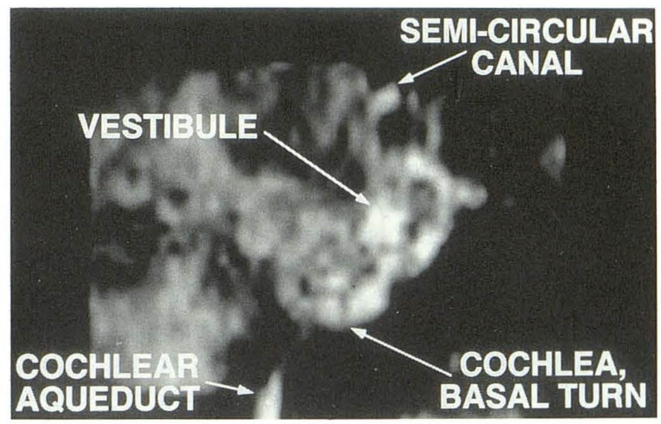

Fig. 4. High-resolution surface-coil maximum-intensity projection image of the internal auditory canal demonstrates the structures of the membranous labyrinth, including the cochlear aqueduct.

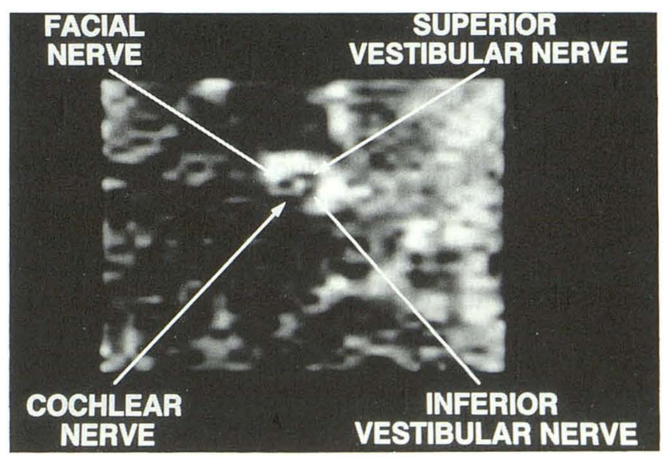

Fig. 5. High-resolution surface-coil sagittal reconstruction reformatted from coronal images. Four nerves are visualized within the internal auditory canal.

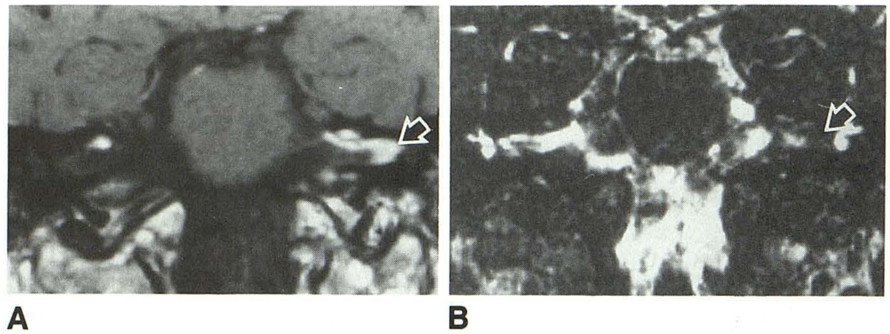

Fig. 6. *A*, T1-weighted image of the internal auditory canal after gadopentetate dimeglumine administration in a patient with a recurrent left acoustic neuroma (*arrow*).

B, Steady-state free precession image of same patient demonstrates a filling defect within the left internal auditory canal (*arrow*), which corresponds to the enhancing lesion.

volunteer demonstrates four nerves within the internal auditory canal (Fig 5).

Discussion

The steady-state free precession pulse sequence assumes a known phase for the transverse magnetization at the end of repetition time period before the next pulse. This is a valid assumption for stationary tissue but not for moving spins. As a result the intensity from the moving spins is less than what it should be because it is not refocused at the acquisition and has a reduced steady-state longitudinal magnetization. Thus these sequences are sensitive to motion and flow. Modest reduction in sensitivity to motion may be noted with the use of gradient-motion rephasing. Endolymph and cerebrospinal fluid within the internal auditory canals have very little flow, so this is not a problem for our application.

The bright signal from the heavily T2-weighted steady-state free precession images gives rise to excellent contrast of the membranous labyrinth. However, the bright signal from cerebrospinal fluid in neighboring cisterns and sulci can obscure inner ear structures on the maximum-intensity projection images. This problem may be minimized by restricting the volume for maximum-intensity projection reconstruction to the area of interest. We are investigating segmentation of the images by region growing to eliminate this problem (5).

We have found steady-state free precession to be useful in the evaluation of patients with sensorineural hearing loss. Small acoustic neuromas appear as a filling defect within the internal auditory canal (Fig 6). We are not advocating the use of this sequence instead of gadolinium-enhanced imaging, but we believe that steady-state free precession may be beneficial for diagnosis in those patients who refuse contrast injection.

The 3-D data set has the potential to help diagnose congenital malformations of the membranous labyrinth. This is important in evaluating sensorineural hearing loss, because the mild forms may not present until adulthood. The complex anatomy of the membranous labyrinth may be revealed by virtue of the 3-D nature of the data.

In summary, we believe steady-state free precession is a useful adjunct technique for the evaluation of patients with sensorineural hearing loss. It has been incorporated into our standard imaging protocol for these patients. The prospective evaluation of the technique will be the subject of a future communication.

Acknowledgment

We thank Gerhard Laub for his help in writing the high-resolution steady-state free precession pulse sequence.

References

1. Brogan M, Chakeres DW, Schmalbrock P. High-resolution 3DFT MR imaging of the endolymphatic duct and soft tissues of the otic capsule. *AJNR Am J Neuroradiol* 1991;12:1–11
2. Tanioka H, Shirakawa T, Machida T, Sasaki Y. Three-dimensional reconstructed MR imaging of the inner ear. *Radiology* 1991;178:141–144
3. Gyngell ML. The application of steady-state free precession in rapid 2DFT NMR imaging: FAST and SSFP sequences. *Magn Reson Imaging* 1988;6:415–419
4. Van der Meulen P, Groen JP, Tinus AMC, Bruntink G. Fast field echo imaging: an overview and calculations. *Magn Reson Imaging* 1998;6:355–368
5. Hu X, Alperin N, Levin DN, Tan KK, Mengeot M. Visualization of MR angiographic data with segmentation and volume-rendering techniques. *J Magn Reson Imaging* 1991;1:539–546